frontiers in Physics

ORIGINAL RESEARCH
published: 13 July 2021
doi: 10.3389/fphy.2021.719293

Random Walks of a Cell With Correlated Speed and Persistence Influenced by the Extracellular Topography

*Kejie Chen and Kai-Rong Qin**

School of Optoelectronic Engineering and Instrumentation Science, Dalian University of Technology, Dalian, China

Cell migration through extracellular matrices is critical to many physiological processes, such as tissue development, immunological response and cancer metastasis. Previous models including persistent random walk (PRW) and Lévy walk only explain the migratory dynamics of some cell types in a homogeneous environment. Recently, it was discovered that the intracellular actin flow can robustly ensure a universal coupling between cell migratory speed and persistence for a variety of cell types migrating in the *in vitro* assays and live tissues. However, effects of the correlation between speed and persistence on the macroscopic cell migration dynamics and patterns in complex environments are largely unknown. In this study, we developed a Monte Carlo random walk simulation to investigate the motility, the search ability and the search efficiency of a cell moving in both homogeneous and porous environments. The cell is simplified as a dimensionless particle, moving according to PRW, Lévy walk, random walk with linear speed-persistence correlation (linear RWSP) and random walk with nonlinear speed-persistence correlation (nonlinear RWSP). The coarse-grained analysis showed that the nonlinear RWSP achieved the largest motility in both homogeneous and porous environments. When a particle searches for targets, the nonlinear coupling of speed and persistence improves the search ability (i.e. find more targets in a fixed time period), but sacrifices the search efficiency (i.e. find less targets per unit distance). Moreover, both the convex and concave pores restrict particle motion, especially for the nonlinear RWSP and Lévy walk. Overall, our results demonstrate that the nonlinear correlation of speed and persistence has the potential to enhance the motility and searching properties in complex environments, and could serve as a starting point for more detailed studies of active particles in biological, engineering and social science fields.

Keywords: random walks, cell migration, correlated speed and persistence, complex topographies, active particles

OPEN ACCESS

Edited by:
Claudia Tanja Mierke,
Leipzig University, Germany

Reviewed by:
Masato S. Abe,
RIKEN Center for Advanced Intelligence Project (AIP), Japan
Luis Diambra,
National University of La Plata, Argentina

****Correspondence:***
Kai-Rong Qin
krqin@dlut.edu.cn

Specialty section:
This article was submitted to Biophysics, a section of the journal Frontiers in Physics

Received: *02 June 2021*
Accepted: *29 June 2021*
Published: *13 July 2021*

Citation:
Chen K and Qin K-R (2021) Random Walks of a Cell With Correlated Speed and Persistence Influenced by the Extracellular Topography. Front. Phys. 9:719293. doi: 10.3389/fphy.2021.719293

1 INTRODUCTION

Eukaryotic cell migration is a crucial process for the normal development and maintenance of organs and tissues. In a wide range of human diseases, such as tumor metastasis, immunological responses and wound healing, cell migration is activated and plays a key role [1–3]. For example, the migratory trajectories and patterns of malignant tumor cells influence the distribution of the secondary tumor, leading to the organotropism phenomenon [4]. Therefore, understanding the cell migration

dynamics and patterns could provide valuable insights about the physiological functions and disease stages.

To access the migration dynamics, cell migrating trajectories in the *in vitro* matrices and live tissues are recorded using live-cell imaging or multi-photon microscopy [5,6]. Early works extracted cell speed v and persistence τ (i.e. the time duration of a straight motion between two switches of directions) from fits of the mean squared displacements (MSDs, $x(t)^2$) using a persistent random walk (PRW) model [6–10]. Specifically, in the PRW model, the MSD follows $2nD(t-\tau_p(1-e^{-t/\tau_p}))$, where n is the dimension of the system, D is the diffusion coefficient, and τ_p is the mean persistence. The PRW model has been widely applied to describe the motion of fibroblasts, epithelial cells and endothelial cells in the 2D and 3D matrices [6–10]. Recent studies showed that the key assumptions made in the PRW model, such as the exponential distribution of persistence, do not hold for all cell types [11–15]. For example, Harris et al. [11] showed that the $CD8^+$ T cells in the brain can migrate for really long distances to target rare pathogens. Metastasizing tumor cells moving along linear fibers or *in vitro* channels acquire superdiffusive motion at long times ($<\boldsymbol{x}(t)^2> \sim t^{\alpha},\ \alpha>1$) [12]. These types of cell migratory motions are better explained by the Lévy walk dynamics rather than the PRW, where the persistence follows a heavy-tailed and power-law distribution ($p(t_p) \sim t_p^{-\mu}$), and μ is the Lévy exponent ($1<\mu<3$).

However, after recording and analyzing trajectories of more cell types, results suggested the PRW and Lévy walk are not general rules for cell migration. For example, Wu et al. [13] showed that the profiles of the moving speed and direction can be anisotropic and self-correlated for fibrosarcoma cells migrating in 2D and 3D collagen-based matrices. Based on a vast amount of migrating trajectories of many cells in various environments collected in the First World Cell Race [16], Maiuri et al. [17] for the first time proposed a universal governing mechanism of cell migration. Specifically, they observed that there is a general trend that faster cells migrate more straight than slower cells, because a large migratory speed leads to the increasing of actin flows and the asymmetry of the concentration profile of polarity cues. Thereby, the cell polarization is stabilized and cell persistence is consequently increased at a large migrating speed. As the actin flow represents a very conserved aspect of cell locomotion, the coupling between cell speed and persistence exists over most cell types migrating via both mesenchymal mode (strong cell-matrix adhesion and elongated cell morphology) and ameboid mode (minimal cell-matrix adhesion and rounded cell morphology). As of yet, the molecular mechanisms that regulate the retrograde actin flows and generate forces to drive the migration have been studied extensively [17–19]. However, effects of the universal coupling between speed and persistence on the macroscopic movement patterns and its functional advantages are still largely unknown.

Moreover, the *in vivo* extracellular microenvironment contains confining pores and channel-like tracks such as the interstitial space between muscle and nerve fibers and the vasculature in the organs [3,20]. These environmental topographies significantly alter cell motility and the optimal moving and searching strategies [14,21–23]. For example, Volpe et al. [24] studied the Lévy walks in the porous media through a Monte Carlo simulation. They found that the concave porous structure alters the optimal moving strategy toward less ballistic and more Brownian strategies. Wondergem et al. [25] measured the trajectories of cells migrating among asymmetrically placed micropillars, and showed that a directed topotactic drift can be generated by the pillar field. Schakenraad et al. [26] further used a PRW model with reflected obstacle boundaries to illustrate how the large-scale topotaxis emerges in the pillar field. Thus, we hypothesize that cells migrating with correlated speed and persistence is also influenced by the environmental topographies. And whether there is an optimal moving strategy among PRW, Lévy walk and random walks with correlated speed and persistence that achieves large cell motility in different environments needs to be further investigated.

To explore the cell locomotion behaviors in complex environmental topographies, in this study we developed a Monte Carlo random walk model to describe four types of migratory strategies, including the PRW, Lévy walk, random walk with linearly correlated speed and persistence (linear RWSP), and random walk with nonlinearly correlated speed and persistence (nonlinear RWSP). In particular, the cell is simplified as a dimensionless particle moving and performing a blind search in a homogeneous environment, in concave and convex porous environments, respectively. The particle motility, the ability and efficiency of searching for targets influenced by the environmental topographies are calculated. We showed that Lévy walk and nonlinear RWSP maintain the superdiffusive motion at long times, while PRW and linear RWSP lead to the normal diffusion ($\alpha = 1$). The superdiffusive motion of Lévy walk and diffusive motion of PRW have also been observed in previous studies [27,28]. The searching ability (i.e. the number of targets found in a fixed time period) is increased due to the correlation between speed and persistence, but the efficiency (i.e. the number of targets found per unit distance) does not. Moreover, in the porous media, the environmental boundaries and barriers restrict particle movement and could generate the subdiffusive motion ($\alpha < 1$). And the searching ability and efficiency are influenced by the target density, the sizes and types of pores as well as the migratory strategies. Overall, in this study, we for the first time quantitatively studied how the correlation between speed and persistence influences the macroscopic cell migration dynamics. We provided a comprehensive comparison among four moving strategies in the homogenous and porous environments, which could help gain insights about functions of immune cells and metastasis cells inside complex *in vivo* environments.

2 METHODS

2.1 The Model

We developed a Monte Carlo based simulation pipeline to describe a cell, which is simplified as a dimensionless particle, moving in a 2D space according to the four strategies, PRW, Lévy walk, linear RWSP and nonlinear RWSP. The coarse grained model ignores the complicated intracellular dynamics, the driving force of the migration as well as the chemotaxis behavior. It only considers

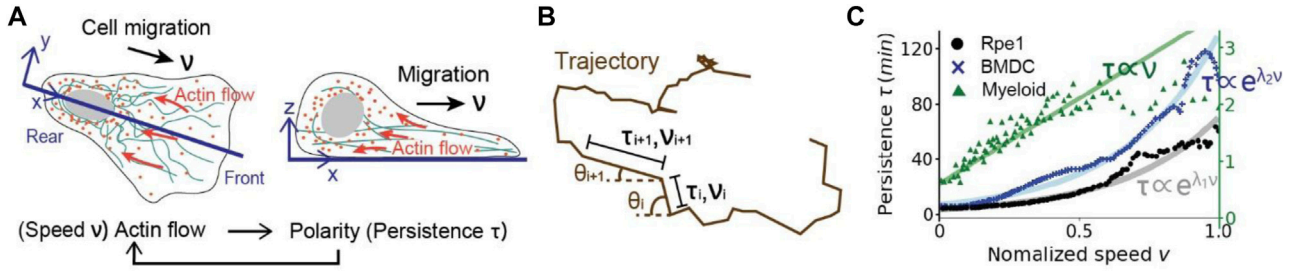

FIGURE 1 | The correlation between migratory speed v and persistence τ is a universal phenomenon existing in the cell migration. **(A)**, Schematics of the cell migration. The correlation between speed and persistence is caused by the intracellular actin flow reinforcing the cell polarity. **(B)**, Schematics of a cell trajectory, which consists a series of straight motions. The time duration of a straight motion i is referred to as persistence τ_i, and the migration speed is v_i and direction is θ_i. **(C)**, Experimentally measured migration speed and persistence of Retinal pigment epithelial cells (Rpe1) (mesenchymal migration model) and bone marrow-derived mice dendritic cells (BMDC) (ameboid migration mode) on a 2D surface, and myeloid cells *in vivo*. Data points are extracted from Figure 1 in reference [17]. For Rpe1 and BMDC cells, the migration speed and persistence are exponentially correlated ($\tau \propto e^{\lambda v}$). For myeloid cells, the persistence increases linearly over the speed ($\tau \propto v$).

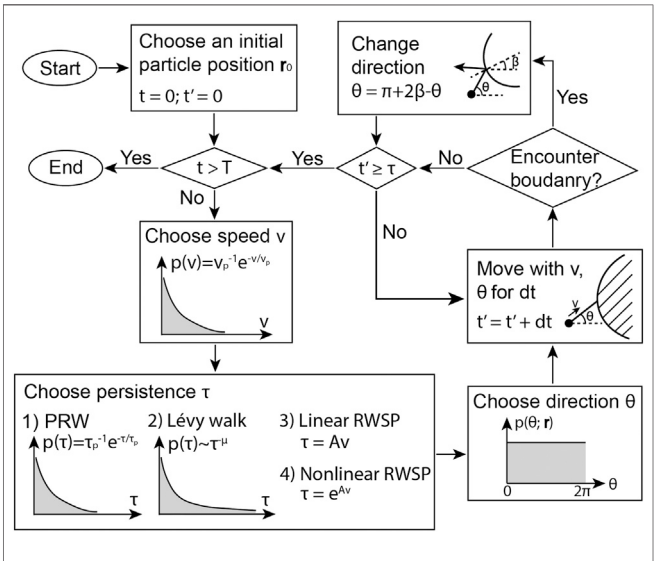

FIGURE 2 | The pipeline of the Monte Carlo simulation of a particle performing PRW, Lévy walk, linear RWSP and nonlinear RWSP. T is the total simulation time. t is the current simulation time. t' is the time the particle has moved along a straight line. dt is the time step of the simulation (i.e. dt = 0.001 s in this study).

core governing physics of a random walker to reduce the computational cost, such that the macroscopic cell motility and patterns over a long time period can be studied based on the model.

Specifically, the 2D random motion of the particle can be described as

$$\frac{d}{dt}x(t) = v_i \cos\theta_i, \tag{1}$$

$$\frac{d}{dt}y(t) = v_i \sin\theta_i, \tag{2}$$

where $(x(t), y(t))$ is the particle position, v_i and θ_i are the magnitude and the direction of the particle velocity during i_{th} time interval (also i_{th} straight motion), where $i = 0, 1, 2, \ldots$ (**Figure 1B**). v_i follows an exponential distribution of mean v_p i.e. $(p(v) = 1/v_p e^{v/v_p})$. θ_i is uniformly distributed in $[0, 2\pi]$ in the homogeneous environment. In the porous media, θ_i is influenced by the interaction between the particle and the walls, which is modeled using boundary conditions described in previous studies [24,29]. The time duration of a straight motion i, which is referred to as the persistence τ_i, follows different distributions for PRW, Lévy walk, linear RWSP and nonlinear RWSP. In the PRW, persistence τ_0, τ_1, τ_2, ... are drawn from an exponential distribution of mean τ_p i.e. $(p(\tau) = 1/\tau_p e^{\tau/\tau_p})$. In the Lévy walk, the persistence follows a Lévy distribution with Lévy exponent μ $(1 < \mu < 3)$. The two limits $\mu \to 1$ and $\mu = 3$ correspond to ballistic and Brownian motions. To draw a random number from a Lévy distribution, calculation steps in a previous study [30] are applied. Briefly, τ_i is calculated as $\tau_i = \sin((\mu-1)X)/(\cos X)^{1/(\mu-1)}(\cos((2-\mu)X)/Y)^{(2-\mu)/(\mu-1)}$, where X is a random variable uniformly distributed in $[-\pi/2, \pi/2]$, and Y is drawn from a unit exponential distribution. In the linear and nonlinear RWSP, the persistence is correlated to the moving speed. From the experimental measurements (**Figure 1C**) [17], the relationship between persistence and speed can be linear or exponential. Thus, in the linear RWSP, let $\tau_i = Av_i$. And in the nonlinear RWSP, $\tau_i = e^{Av_i}$, where A is a model parameter.

The Monte Carlo simulation pipeline is shown in **Figure 2**. At the beginning of a straight motion, the particle speed, persistence and moving direction are chosen. In the following each time step dt (i.e. dt = 0.001 s in this study), the particle moves vdt distance along θ direction. When the particle encounters environmental boundaries, which is modeled as reflected walls, it changes moving direction according to $\theta_{\text{new}} = \pi + 2\beta - \theta$, where $\beta = \arctan(y_c - y_i/x_c - x_i)$, (x_c, y_c) is the center of the curvature of the boundary, (x_i, y_i) is the position where the particle encounters the boundary (**Figure 3**).

2.2 Quantification of the Dynamics

The cell migration dynamics is characterized by its motility, and its ability and efficiency to reach a targeting position or to find a target such as a pathogen. The motility is mainly described by the

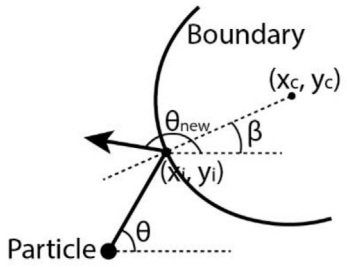

FIGURE 3 | Schematics of the particle changing moving direction from θ to θ_{new} at the boundary.

TABLE 1 | Parameters of the circular pores of the concave and convex porous medium. N_{pores} is the number of circular pores. r_P is the average radius, and σ_P is the standard deviation of the pore radius. Units of r_P and σ_P are pixels.

Concave				Convex			
Environment	N_{pores}	r_P	σ_P	**Environment**	N_{pores}	r_P	σ_P
1	35	120	20	1	20	120	20
2	70	90	15	2	30	90	15
3	140	60	10	3	50	60	10
4	280	30	5	4	100	30	5
5	500	15	2.5	5	200	15	2.5

MSDs and the distributions over time. The MSDs are calculated as $<\boldsymbol{x}(t)^2> = \sum_{j=1}^{n_p} [\boldsymbol{x_j}(t) - \boldsymbol{x_j}(0)]^2$, where n_p is the number of particles simulated (i.e. $n_p = 10000$ in this study), $\boldsymbol{x_j}(t)$ is the position of particle j at time t. The MSD curves can be approximated by $<\boldsymbol{x}(t)^2> = 4D_\alpha t^\alpha$ [31], where the motion is superdiffusive when $\alpha > 1$, diffusive when $\alpha = 1$, and subdiffusive when $\alpha < 1$. D_α is the equivalent diffusion coefficient. In the homogeneous space, the particle motion and its distribution are isotropic. For simplicity, the 1D particle distribution along the center line of the 2D homogeneous space is compared with a Gaussian distribution. The Jensen Shannon divergence (JSD) is used to quantitatively describe the difference between the particle distribution and a Gaussian distribution, which is defined as [32].

$$\mathrm{JSD} = \frac{1}{2}\left(\int p(x)\log\frac{p(x)}{G(x)}dx + \int G(x)\log\frac{G(x)}{p(x)}dx \right), \quad (3)$$

Where $p(x)$ is the particle distribution, and $G(x)$ is a Gaussian distribution. When the particle distribution is similar to a Gaussian distribution, JSD is close to 0.

To quantify the ability and efficiency for a cell to reach targeting positions or to find targets, the average numbers of targets found in a fixed time period and per unit migratory distance are calculated. Specifically, targets with density ρ are uniformly distributed in the 2D space where the particle can access. When the distance between the target and the particle is less than $r_s = 3$ in normalized units ($n.u.$), the target is assumed to be found by the particle. Finding a target does not influence the moving direction and duration of the particle. The targets are dimensionless and scarce i.e. with density ($\rho \ll r_s^{-2}$). The targets are non-regenerative which means that a target will disappear once it is found by the particle. For example, a pathogen is a non-regenerative target because it will be cleaned up by the immune T cell once it is found by the cell. In the study, $\langle N_h \rangle$ in the homogeneous environment and $\langle N_p \rangle$ in the porous media are the mean target numbers found in 150 s. The larger $\langle N_h \rangle$ and $\langle N_p \rangle$ are, the greater ability for the particle to find more targets. $\langle \eta_h \rangle$ and $\langle \eta_p \rangle$ are the mean target numbers found per unit distance in the homogeneous and porous environments. For example, $\langle \eta_h \rangle$ are calculated as $\langle \eta_h \rangle = 1/n_p \sum_{k=1}^{n_p} N_{hk}/L_k$, where n_p is the particle number ($n_p = 10000$), N_{hk} is the number of targets found by particle k in 150 s, and L_k is the distance particle k moves in 150 s. When the energy a cell takes to move for a unit distance is maintained as constant, $\langle \eta_h \rangle$ and $\langle \eta_p \rangle$ can be used to represent the efficiency of searching for targets (i.e. how many targets can be found by consuming the same amount of energy).

2.3 Simulation Method and Model Parameters

In the simulation, a 1000×1000 pixels^2 space with period boundaries are used. The total simulation time is set as 150 s. The time step is set as $dt = 0.001$. Particle speed follows an exponential distribution with mean speed $v_p = 0.5$ pixels/s if not specified. For the PRW, the moving persistence follows an exponential distribution with mean value $\tau_p = 1.0\,s$. Lévy exponent is chosen as $\mu = 2$ if not specified. For the linear RWSP, we set $\tau = v$. And for the nonlinear RWSP, let $\tau = e^v$ if not specified. Trajectories of $n_p = 10000$ particles are calculated.

To generate a porous environment, N_{pores} circular pores are randomly and uniformly distributed in the 2D space. For the concave porous medium, the particle moves inside the circular pores. For the convex porous medium, the particle moves outside the circular pores. The radius of circular pores follows a Gaussian distribution with mean r_p and standard deviation σ_P, listed in **Table 1**. The boundaries of the circular pores are reflective. To avoid the particle being trapped inside the isolated pores in the concave porous medium, a large number of pores (a large N_{pores}) is applied to ensure pores are connected, especially when the pore radius is small. For the convex porous medium, to avoid the particle being trapped between several circular pores (obstacles), a small N_{Pores} is used such that the accessible areas to the particle are connected, especially when r_P is large. Note that, because the surrounding boundaries of the square space is period, the accessible area to the particle is always infinite. In addition, the target density is calculated as ρ = total number of targets / area accessible to the particle.

3 RESULTS

3.1 Dynamics in a Homogeneous Environment

In a homogeneous environment, the directional preference is isotropic and the speed follows an exponentially decaying

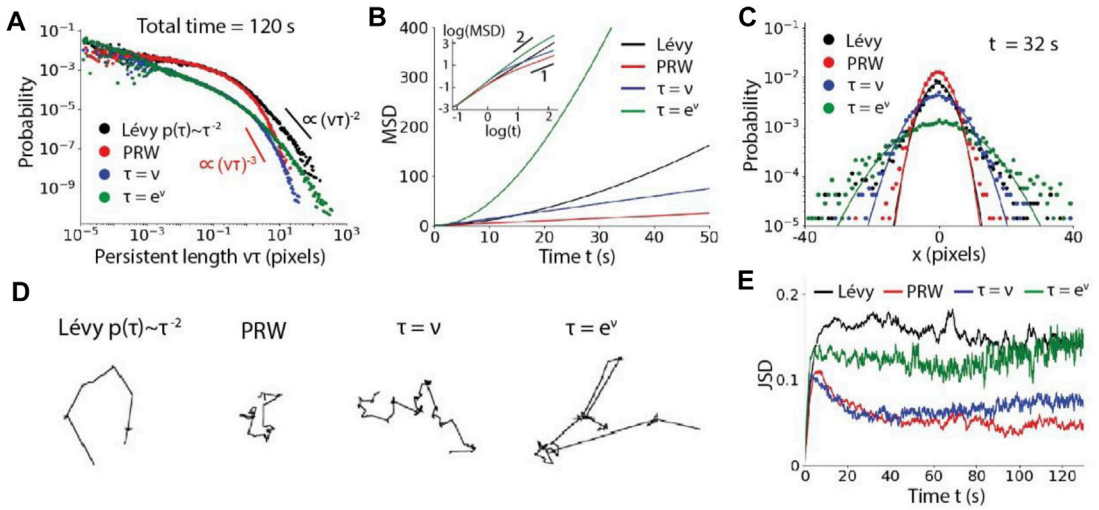

FIGURE 4 | Particle motility influenced by the moving strategies in a homogeneous environment. **(A)**, Distributions of persistent length ($v\tau$) of PRW, Lévy walk, linear RWSP ($\tau = v$) and nonlinear RWSP ($\tau = e^v$), whose tails can be well-approximated by a power law. **(B)**, Mean square displacements (MSDs) over time. **(C)**, Particle distributions at $t = 32\,s$. Dots represent the particle distributions. Solid lines represent Gaussian distributions. **(D)**, Example trajectories. **(E)** Jensen Shannon divergence (JSD) over time, which indicates the difference between the particle distribution and a Gaussian distribution.

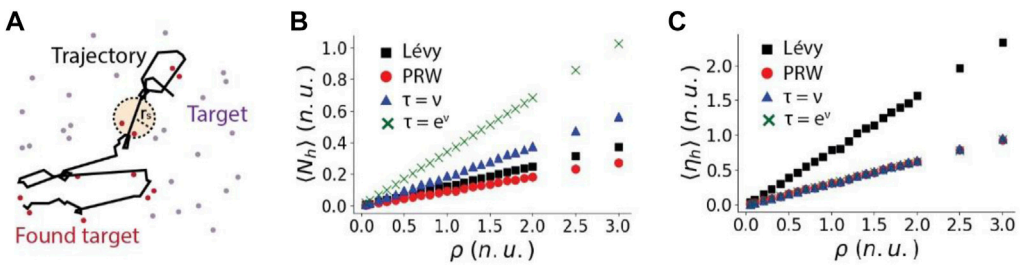

FIGURE 5 | The search ability $\langle N_h \rangle$ and efficiency $\langle \eta_h \rangle$ of a particle influenced by the moving strategies in the homogeneous environment. **(A)**, Schematic illustration of a particle searching for targets. When the distance between the target and the particle is less than $r_s = 3$ in normalized units (n.u.), the target is assumed to be found by the particle. **(B)**, The number of targets found by the particle $\langle N_h \rangle$ over the target density ρ in the homogeneous space. **(C)**, The search efficiency $\langle \eta_h \rangle$ over the target density ρ. The search efficiencies of PRW, linear RWSP and nonlinear RWSP overlaps.

probability distribution. As expected, the power-law distribution of the persistence in the Lévy walk ($\mu = 2$ if not specified) leads to long straight movements and slowly decaying distribution of persistent length $v\tau$. The nonlinear correlation of speed and persistence ($\tau = e^v$ if not specified) also generates long straight motions and the tail of its distribution decays slower than the Lévy walk. This happens because a particle can move slowly for a long persistence and eventually acquire a small persistent length in the Lévy walk. But a long persistence always corresponds to a large speed in the nonlinear RWSP. In addition, PRW and linear RWSP ($\tau = v$ if not specified) switch moving directions frequently, and have shorter straight motions (**Figures 4A,D**). Therefore, though all the moving strategies show superdiffusive motion at short times (e.g. $t < 5\,s$), only the Lévy walk [28] and the nonlinear RWSP can maintain the superdiffusion at long times. PRW [27] and linear RWSP perform diffusive motion at long times. Among the four migrating strategies, the particle has the largest motility moving with nonlinear RWSP, as the MSD curve increases significantly faster than the others (**Figure 4B**). Particle distributions (also the displacement probability distributions) at the center line of the 2D space suggest that tails of the Lévy walk and the nonlinear RWSP decay slower than Gaussian distributions (**Figure 4C**). The divergence of the particle distribution from a Gaussian distribution is quantitatively characterized using the relative entropy (i.e. by calculating the Jensen Shannon divergence over time) (**Figure 4E**). These results show that PRW and linear RWSP become more Brownian-like at long times, while Lévy walk and nonlinear RWSP are anomalous.

What is the best moving strategy for a cell to search for randomly located pathogens or to reach targeting tissue spots? It is long believed that Lévy walk reduces oversampling and is more efficient in finding targets than PRW when targets are sparse

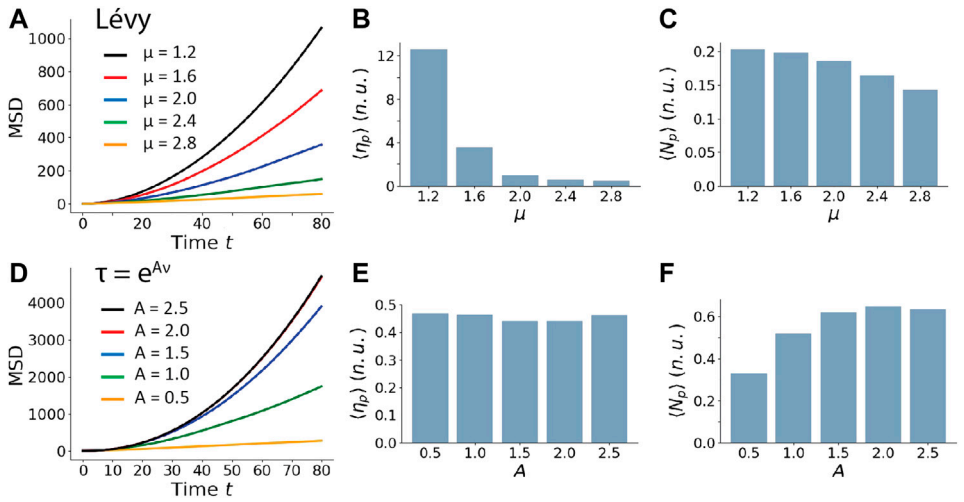

FIGURE 6 | The influence of model parameters of Lévy walk and nonlinear RWSP on the particle motility, searching ability and efficiency in a homogeneous medium. For a particle performing the Lévy walk, **(A)**, the MSD, **(B)**, the search efficiency $\langle \eta_p \rangle$, **(C)**, the searching ability $\langle N_p \rangle$ influenced by the Lévy exponent μ. For a particle performing the nonlinear RWSP, **(D)**, the MSD, **(E)**, the search efficiency $\langle \eta_p \rangle$, and **(F)**, the searching ability $\langle N_p \rangle$ influenced by the coefficient A in the speed-persistence relationship $\tau = e^{Av}$. The target density ρ in **(B, C, E)** and **(F)** is 1.5. (*n.u.*).

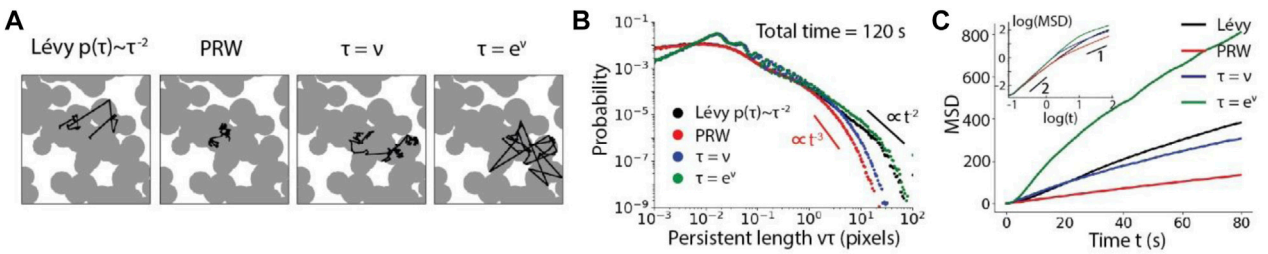

FIGURE 7 | Particle mobility influenced by the moving strategies in a concave porous environment. **(A)**, Example trajectories of Lévy walk, PRW, linear RWSP ($\tau = v$) and nonlinear RWSP ($\tau = e^v$). Gray areas are inside the pores and accessible to the particle. White areas are inaccessible. Black lines are the particle trajectories. **(B)**, The distribution of persistent length, whose tails are well-approximated by power laws with cutoff at large persistent lengths. **(C)**, Mean square displacements (MSDs) over time.

[33,34]. But whether the correlation between speed and persistence can further improve searching for targets is not known. Thus, we compared the ability and efficiency of searching for targets among PRW, Lévy walk, linear RWSP and nonlinear RWSP (**Figure 5A**). The search ability is represented by the average number of targets found by the particle in a fixed time period, denoted as $\langle N_h \rangle$. The larger $\langle N_h \rangle$ is, the more targets that the particle is able to find. The search efficiency is the average number of targets found per unit distance, denoted as $\langle \eta_h \rangle$. If the energy that a cell consumes to migrate for a unit distance remains as constant, $\langle \eta_h \rangle$ indicates the energy efficiency of finding targets. **Figure 5B** shows that a particle moving according to the nonlinear RWSP has the greatest ability of finding targets over a wide range of target densities. The search ability of the linear RWSP is also larger than the Lévy walk. PRW finds the smallest number of targets in a fixed time. The results agree with the fact that the nonlinear RWSP achieves many long straight motions and have the largest motility, as shown in **Figure 4**. However, interestingly, we found that the search efficiency of the nonlinear RWSP is lower than the Lévy walk. In fact, the search efficiency of the nonlinear and linear RWSP are similar to the PRW (**Figure 5C**). In other words, the nonlinear RWSP scarifies the energy efficiency to find more targets in a fixed time period. The large motility and search ability of the nonlinear RWSP is due to both the increasing of the average moving speed and the nature of the movements. Specifically, at the beginning of a straight motion, the moving speeds of both the Lévy walk and the nonlinear RWSP are sampled from the same exponential distribution $(p(v) = v_p^{-1} e^{v/v_p})$, $v_p = 0.5$ in **Figures 4**, **5**. However, because a fast-moving particle tends to maintain the large speed for a long time in nonlinear RWSP, the average moving speed in a fixed time period (say 100 s) of the nonlinear RWSP is larger than the Lévy walk (**Supplementary Table S1** in

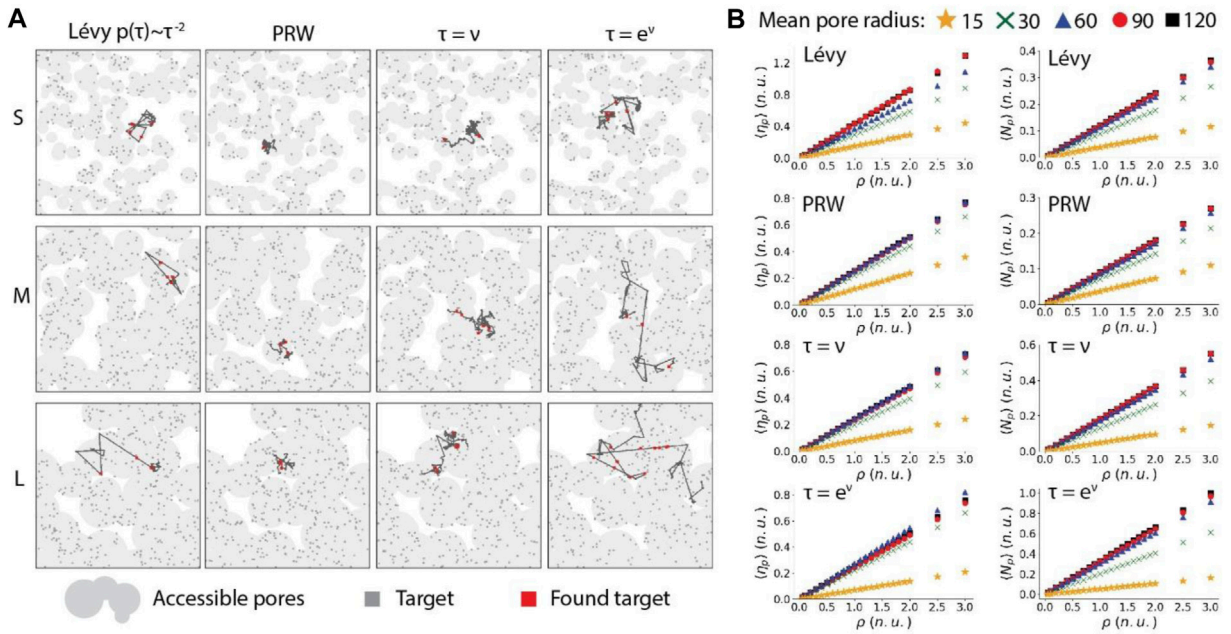

FIGURE 8 | The search ability and efficiency of a particle influenced by different moving strategies in the concave porous environments. **(A)**, Example trajectories of Lévy walk, PRW, linear RWSP ($\tau = v$) and nonlinear RWSP ($\tau = e^v$) in the concave porous media with different pore sizes. S represents small pore size (r_p = 30 pixels, σ_p = 5 pixels), M represents intermediate pore size (r_p = 60 pixels, σ_p = 10 pixels), and L represents large pore size (r_p = 90 pixels, σ_p = 15 pixels). Light gray areas are accessible to the particle and white areas are inaccessible. Gray dots are the targets, and red dots are the targets found by the particle. Dark gray lines are particle trajectories. **(B)**, The search ability $\langle N_p \rangle$ and efficiency $\langle \eta_p \rangle$ over target densities ρ influenced by the pore sizes. Dynamics in a convex porous environment.

the supplementary materials). When the average moving speeds of the Lévy walk and the nonlinear RWSP are similar, the motility, search ability and efficiency of the particle are further compared (**Supplementary Figure S1** in the supplementary materials). In particular, the average speed of the Lévy walk with $v_p = 2.0$ ($v_p = 3.0$) is similar to the average speed of the nonlinear RWSP with $v_p = 0.7$ ($v_P = 2.0$) in 100 s. But for these four cases, the MSD of the nonlinear RWSP still increases faster than the Lévy walk and the search ability is larger. And the search efficiency of the nonlinear RWSP is smaller than the Lévy walk (**Supplementary Figure S1**).

As suggested by the experimental results in **Figure 1C**, the coefficient A in the speed-persistence relationship $\tau = e^{Av}$ varies over different cell types and environmental matrices. And in the Lévy walk, the Lévy exponent μ can take values between 1 and 3. To better understand the influence of the coefficient A and the Lévy exponent μ on the moving dynamics, the MSD, searching ability and efficiency over different values of A and μ are calculated and compared (**Figure 6**). The motility (MSD), searching ability $\langle N_p \rangle$ and searching efficiency $\langle \eta_p \rangle$ increase when μ decreases or A increases. Overall, the MSD and the searching ability $\langle N_p \rangle$ of the nonlinear RWSP is significantly larger than the Lévy walk. The searching efficiency $\langle \eta_p \rangle$ of the Lévy walk is large when μ is closer to 1 (the motion is close to ballistic). $\langle \eta_p \rangle$ of the Lévy walk decreases rapidly to a level lower than $\langle \eta_p \rangle$ of the nonlinear RWSP when μ becomes closer to 3 (the motion becomes Brownian-like). The searching efficiency of the nonlinear RWSP is less influenced by the coefficient A (**Figure 6**).

3.2 Dynamics in a Concave Porous Environment

To understand how the complexity of the environment influences the motility, the search ability and the search efficiency of a particle moving with different strategies, we then consider a particle in a heterogeneous topography. Specifically, the 2D space is now a concave porous medium composed of uniformly distributed circular interconnected pores with mean radius r_p and standard deviation σ_p, where $r_p \gg r_s$. The characteristic size of a cluster of pores is much larger than the displacement of the particle during the total simulation time. Trajectories of the particle moving with PRW, Lévy walk, linear RWSP and nonlinear RWSP are shown in **Figure 7A**. Though really long straight movements are interrupted by the reflections at the porous boundaries, average lengths of a straight motion (i.e. the persistent length) of the Lévy walk and the nonlinear RWSP are still larger than the PRW and the linear RWSP (**Figure 6B**). As a result, the motility, characterized by the MSDs, of the nonlinear RWSP and Lévy walk are large (**Figure 7C**). In addition, due to the confinement of the pores, distributions of the persistent length have cutoff at large values, especially for Lévy walk and nonlinear RWSP. And the particle moving with the four strategies performs superdiffusive motion at

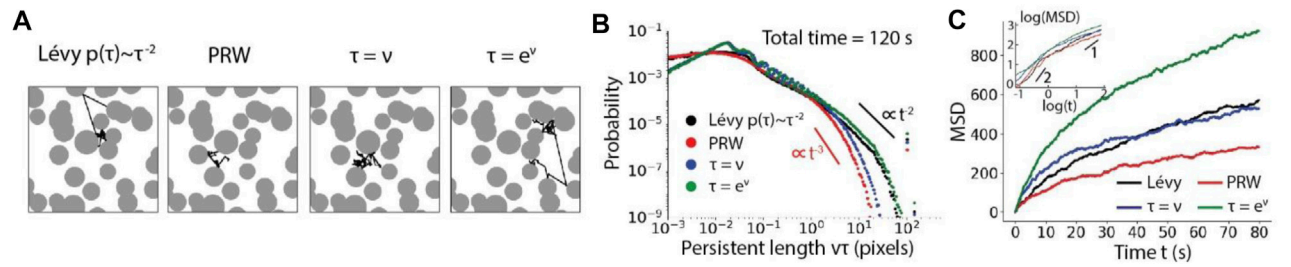

FIGURE 9 | Particle motility influenced by the moving strategies in a convex porous environment. **(A)**, Example trajectories of Lévy walk, PRW, linear RWSP and nonlinear RWSP reflected by the circular obstacles. **(B)**, The distribution of the persistent length, whose tails are approximated by power laws with cutoff at large values. **(C)**, MSD curves over time. The particle motion is superdiffusive at short times and subdiffusive at long times.

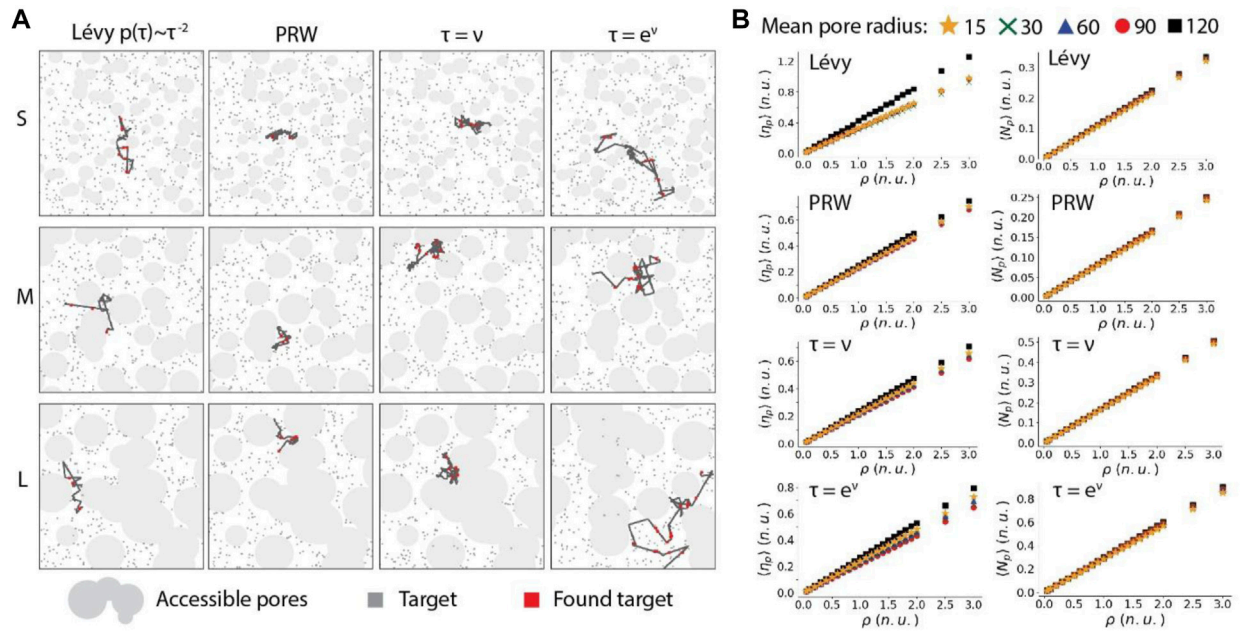

FIGURE 10 | The search efficiency of a particle influenced by the moving strategies in the convex porous environments. **(A)**, Examples of a particle moving according to the Lévy walk, PRW, linear RWSP and nonlinear RWSP in the porous media and searching for targets. S represents small pore size (r_p = 30 pixels, σ_p = 5 pixels), M represents intermediate pore size (r_p = 60 pixels., σ_p = 10 pixels), and L represents large pore size (r_p = 90 pixels, σ_p = 15 pixels). Light gray areas are accessible to the particle and white areas are inaccessible. Gray dots are the targets, and red dots are the targets found by the particle. Dark gray lines are particle trajectories. **(B)**, The search ability and efficiency over the target density ρ influenced by the pore sizes.

short time and diffusive motion at long times. Overall, the concave porous topographies have smaller influence on the PRW and linear RWSP compared with the homogeneous conditions, but restrict the motions of the Lévy walk and the nonlinear RWSP. Moreover, due to the confinement of the pores, Lévy walk with $\mu < 1.6$ and nonlinear RWSP with $A > 2.0$ are less influenced by the parameters μ and A. The motility and search ability of the nonlinear RWSP are still larger than the Lévy walk. And the search efficiency of the Lévy walk with μ close to 1 is the largest (**Supplementary Figure S2** in the supplementary materials).

Next, we investigated the search ability and efficiency of a particle influenced by the concave porous topographies. Specifically, numbers of targets found by the particle in 150 s and per unit distance are calculated over different pore sizes and target densities. **Figure 8A** shows the representative trajectories of the particles in small-size, intermediate-size and large-size porous media. As expected, the confinement is significant when the pore size is small for the Lévy walk and nonlinear RWSP. Therefore, the searching ability $\langle N_p \rangle$ decreases over the pore size (**Figure 8B**). The decreasing of the search ability over the pore size is consistent among the four moving strategies. In particular, while linear and nonlinear RWSP can still maintain a relatively large search ability within large connected pores, the search ability of all the four strategies decreases to a similar level when the average pore radius is only 15 pixels. For the search

efficiency $\langle \eta_p \rangle$, Lévy walk, PRW and linear RWSP decreases monotonically over the pore size due to the confinement of the boundaries. Interestingly, we discovered a small increasing of the search efficiency within the intermediate-size pores for a particle moving with the nonlinear RWSP. It indicates that long straight movements are broken into several short segments by the porous boundaries, which reduces the search ability but can slightly improve the efficiency. Effects of the pore size on the search efficiency of the Lévy walk is the most significant. Thus, though the search efficiency of the Lévy walk is larger than the other three strategies in a homogeneous environment and a concave porous environment with large pore size, the efficiency of the nonlinear RWSP becomes similar the Lévy walk when the pore size is intermediate and small. Moreover, both the search ability and efficiency increase linearly over the target densities. Overall, the results suggest that the nonlinear RWSP could be an optimal moving strategy in a concave porous media with intermediate pore size, as it achieves relatively large search ability and efficiency.

3.3 Dynamics in a convex porous environment

Lastly, we considered a porous medium with convex topographies. In the convex porous environment as shown in **Figure 9A**, a particle moves in the white space and is reflected by the gray circular obstacles, which are randomly and uniformly distributed in the space. The density of circular obstacles is ρ, mean radius is r_p ($r_p \gg r_s$) and standard deviation is σ_p. In the convex porous media, distributions of the persistent length decay rapidly at the tails, and the motion of the particle becomes subdiffusive at long times (**Figures 9B,C**). Particularly, the increasing of the MSD of the Lévy walk is reduced to a similar level as the linear RWSP. The subdiffusive motion of the particle can be caused by the narrow spaces between the circular obstacles which transiently trap the particle (**Figure 9A**). In the convex porous medium, the influence of the Lévy exponent μ and speed-persistence correlation coefficient A is reduced because long straight movements are interrupted by the obstacle boundaries. When $\mu < 2.0$ or $A > 1.0$, the particle motility and search ability maintain at a similar level. When μ is close to 1, the search efficiency of the Lévy walk is the largest (**Supplementary Figure S3** in the supplementary materials).

In the convex porous media, examples of a particle searching for targets with small, intermediate and large obstacle sizes are shown in **Figure 10A**. Because the particle is probable to be reflected back and forth within the narrow space between several obstacles, the area that the searcher can cover in a fixed time period is reduced (**Figure 10A**). The results show that the size of pores has a small influence on the searching ability of the particle, regardless of the moving strategies and the target densities (**Figure 10B**). Similar to the dynamics in the homogeneous and concave porous environments, the nonlinear and linear RWSP can find relatively larger numbers of targets than the Lévy walk and PRW. Interestingly, we found that the search efficiency is the largest when the circular obstacles have the largest mean radius of 120 pixels for all the four types of moving strategies (**Figure 10B**). For the other obstacle sizes (i.e. their mean radiuses range from 15 pixels to 90 pixels), the search efficiencies of the Lévy walk and the PRW are not influenced by the obstacle size. And the search efficiencies for the linear and nonlinear RWSP slightly decrease when the obstacle size increases (**Figure 10B**). The lowest search efficiency in the intermediate-size porous environment is caused by many narrow channel-like spaces that trap the particle inside. In general, influenced by the large-size obstacles, Lévy walk has the highest search efficiency. And among the intermediate-size and small-size obstacles, the search efficiencies of the nonlinear RWSP and Lévy walk are relatively large. In addition, both the search ability and efficiency increases linearly over the target densities (**Figure 9B**). Overall, in the convex topographies, the nonlinear RWSP also show advantageous properties among the four moving strategies.

4 DISCUSSION

In this study, we developed a coarse-grained random walk model to study the dynamics of a cell, which is represented by a dimensionless particle, moving in the homogeneous and porous media with correlated speed and persistence. The motility (i.e. MSDs and distributions), the search ability (i.e. the number of targets found in a fixed time period) and the search efficiency (i.e. the number of targets found per unit distance) are calculated and compared among the four moving strategies, including the Lévy walk, PRW, linear RWSP and nonlinear RWSP. We show that when the speed and persistence are exponentially correlated (nonlinear RWSP), the motility of the particle is the largest in both homogeneous and porous environments. Compared with the Lévy walk which is believed to be an efficient searching method in many studies [28,33], our results demonstrate that the nonlinear RWSP has a larger search ability but sacrifices the search efficiency. Moreover, the concave and convex porous topographies modify the dynamics of the Lévy walk and nonlinear RWSP significantly by interrupting long straight movements and transiently trapping the particles within the narrow pores or channel-like spaces. Our model and analysis provide fundamental evidences and insights about how the correlation between cell speed and persistence improves the cell locomotion behaviors. Our model has the potential to be further used to understand the influence of disease-impaired speed and persistence on cell migration.

There were previous models that describe cell migration based on the changing of cell configuration or the protrusion force, resistance force and friction experienced by the cell [34–37]. For example, the cellular potts model considers the adhesion to the matrix and the resistance to the volume change, and predicts the migration by minimizing the energy of a particular cell configuration [34]. Yang et al. includes the protrusion force generated by the filament network, and modeled the chemotaxis behavior when the chemoacttractant stimulation changes the number of filaments and modifies the protrusion force [35]. To uncover more realistic migratory dynamics and improve the prediction power and accuracy, the effects of cell

configuration and the mechanical forces acting on the cell can be further included in the proposed model.

Several aspects in our model could influence the moving dynamics of the particle. First, in this work, reflective boundary conditions of the porous structures are implemented. Specifically, when the particle reaches the porous boundaries, it will immediately change the moving direction and move away from the boundary. This scenario is discovered in biological and artificial microswimmers such as Janus particles [38] and elementary robots [39]. The interactions between a cell and a wall or other repulsive sources can be more complicated. For example, a cell can migrate along the wall boundaries instead of migrating away [40]. Sometimes, the cell can penetrate the wall barriers. For example, the circulating tumor cells can actively attach to the vessel wall and extravasate to the surrounding matrix [41]. Therefore, other physiological-relevant boundary conditions need to be considered in the future studies, which could potentially influence the optimality of the random walks with nonlinearly correlated speed and persistence. Second, in reality, the moving and searching time is generally finite. Therefore, the particle is allowed to move in the environment for a finite simulation time in this study. However, it would be interesting to investigate particle motion in the environment in the limit of infinite times from a fundamental perspective. Other important statistics such as the survival probability and first passage time can be understood accordingly. Lastly, other moving strategies, such as the intermittent random walk and correlated random walk, have been observed in biological and ecological systems [42–44]. For example, in the intermittent random walk, a particle is assumed to randomly switch between Brownian diffusion and ballistic motion [42]. Furthermore, a particle can also perform a mixture of many types of motions, such as a mixture of Lévy walk, PRW and nonlinear RWSP. It would also be interesting to further investigate if the combination of several moving strategies is advantageous in complex environmental topographies.

The model and results are relevant for all random moving and searching problems at various length and time scales, such as the intracellular protein diffusion, bacteria spreading, animal foraging and human travelling. As suggested by our results that the correlation between speed and persistence could potentially improve the motility and searching properties, these results could inspire studies of the novel migratory statistics and rules in many other science and engineering fields.

DATA AVAILABILITY STATEMENT

The original contributions presented in the study are included in the article/supplementary files, further inquiries can be directed to the corresponding author/s.

AUTHOR CONTRIBUTIONS

KC: Conceptualization, Methodology, Software, Validation, Investigation, Formal analysis, Data curation, Writing – original draft, Writing – review & editing; K-RQ: Conceptualization, Methodology, Writing–review & editing, Supervision, Project administration, Funding acquisition, Resources, Investigation.

FUNDING

This research is supported by the Fundamental Research Funds for the Central Universities in China (DUT21RC(3)044 and DUT20YG113).

SUPPLEMENTARY MATERIAL

The Supplementary Material for this article can be found online at: https://www.frontiersin.org/articles/10.3389/fphy.2021.719293/full#supplementary-material

REFERENCES

1. Krummel MF, Bartumeus F, and Gérard A "T Cell Migration, Search Strategies and Mechanisms". *Nat Rev Immunol* 16, no. 3 (2016): 193, 201. doi:10.1038/nri.2015.16
2. Yamada KM, and Sixt M. "Mechanisms of 3D Cell Migration." *Nat Rev Mol Cel Biol* 20, no. 12 (2019): 738–52. doi:10.1038/s41580-019-0172-9
3. Paul CD, Mistriotis P, and Konstantopoulos K. "Cancer Cell Motility: Lessons from Migration in Confined Spaces." *Nat Rev Cancer* 17, no. 2 (2017): 131, 40. doi:10.1038/nrc.2016.123
4. Lo HC, and Zhang XH-F. "EMT in Metastasis: Finding the Right Balance." *Develop Cel* 45, no. 6 (2018): 663–5. doi:10.1016/j.devcel.2018.05.033
5. Hackl MJ, Burford JL, Villanueva K, Lam L, Suszták K, Schermer B, et al. "Tracking the Fate of Glomerular Epithelial Cells *In Vivo* Using Serial Multiphoton Imaging in New Mouse Models with Fluorescent Lineage Tags." *Nat Med* 19, no. 12 (2013): 1661–6. doi:10.1038/nm.3405
6. Wu P-H, Giri A, and Wirtz D. "Statistical Analysis of Cell Migration in 3D Using the Anisotropic Persistent Random Walk Model." *Nat Protoc* 10, no. 3 (2015): 517–27. doi:10.1038/nprot.2015.030
7. Gorelik R, and Gautreau A. "Quantitative and Unbiased Analysis of Directional Persistence in Cell Migration." *Nat Protoc* 9, no. 8 (2014): 1931, 43. doi:10.1038/nprot.2014.131
8. Campos D, Méndez V, and Llopis I. "Persistent Random Motion: Uncovering Cell Migration Dynamics." *J Theor Biol* 267, no. 4 (2010): 526–34. doi:10.1016/j.jtbi.2010.09.022
9. Selmeczi D, Li L, Pedersen LII, Nrrelykke SF, Hagedorn PH, Mosler S, et al. "Cell Motility as Random Motion: A Review". *Eur Phys J Spec Top* 157, no. 1 (2008): 1–15. doi:10.1140/epjst/e2008-00626-x
10. Stokes CL, Lauffenburger DA, and Williams SK. "Migration of Individual Microvessel Endothelial Cells: Stochastic Model and Parameter Measurement." *J Cel Sci* 99, no. 2 (1991): 419–30. doi:10.1242/jcs.99.2.419
11. Harris TH, Banigan EJ, Christian DA, Konradt C, Elia D, Tait W, et al. "Generalized Lévy Walks and the Role of Chemokines in Migration of Effector CD8+ T Cells." *Nature* 486, no. 7404 (2012): 545-548. doi:10.1038/nature11098
12. Huda S, Weigelin B, Wolf K, Tretiakov KV, Polev K, Gary W, et al. "Lévy-like Movement Patterns of Metastatic Cancer Cells Revealed in Microfabricated Systems and Implicated *In Vivo*." *Nat Commun* 9, no. 1 (2018): 1–11. doi:10.1038/s41467-018-06563-w
13. Wu P-H, Giri A, Sun SX, and Wirtz D. "Three-dimensional Cell Migration Does Not Follow a Random Walk." *Proc Natl Acad Sci* 111, no. 11 (2014): 3949–54. doi:10.1073/pnas.1318967111
14. Baumgart F, Schneider M, and Schütz GJ. "How T Cells Do the "Search for the Needle in the Haystack." *Front Phys* 7 (2019): 11. doi:10.3389/fphy.2019.00011

15. Banigan EJ, Harris TH, Christian DA, Hunter CA, and Liu AJ. "Heterogeneous CD8+ T Cell Migration in the Lymph Node in the Absence of Inflammation Revealed by Quantitative Migration Analysis." *Plos Comput Biol* 11, no. 2 (2015): e1004058 doi:10.1371/journal.pcbi.1004058
16. Maiuri P, Terriac E, Paul-Gilloteaux P, Vignaud T, McNally K, Onuffer J, et al. "The First World Cell Race." *Curr Biol* 22, no. 17 (2012): R673–R675. doi:10.1016/j.cub.2012.07.052
17. Maiuri P, Rupprecht J-F, Wieser S, Ruprecht V, Bénichou O, Carpi N, et al. "Actin Flows Mediate a Universal Coupling between Cell Speed and Cell Persistence." *Cell* 161, no. 2 (2015): 374–86. doi:10.1016/j.cell.2015.01.056
18. Petrie RJ, Doyle AD, and Yamada KM. "Random versus Directionally Persistent Cell Migration." *Nat Rev Mol Cel Biol* 10, no. 8 (2009): 538–49. doi:10.1038/nrm2729
19. Leithner A, Eichner A, Müller J, Reversat A, Brown M, Schwarz J, et al. "Diversified Actin Protrusions Promote Environmental Exploration but Are Dispensable for Locomotion of Leukocytes." *Nat Cel Biol* 18, no. 11 (2016): 1253–9. doi:10.1038/ncb3426
20. Charras G, and Sahai E. "Physical Influences of the Extracellular Environment on Cell Migration." *Nat Rev Mol Cel Biol* 15, no. 12 (2014): 813–24. doi:10.1038/nrm3897
21. Park J, Kim D-H, and Levchenko A. "Topotaxis: a New Mechanism of Directed Cell Migration in Topographic ECM Gradients." *Biophysical J* 114, no. 6 (2018): 1257–63. doi:10.1016/j.bpj.2017.11.3813
22. Reversat A, Gaertner F, Merrin J, Stopp J, Tasciyan S, Aguilera J, et al. "Cellular Locomotion Using Environmental Topography." *Nature*, 582 (2020): 582–585. doi:10.1038/s41586-020-2283-z
23. Lee H-pyo, Alisafaei F, Adebawale K, Chang J, Shenoy VB, and Chaudhuri O. "The Nuclear Piston Activates Mechanosensitive Ion Channels to Generate Cell Migration Paths in Confining Microenvironments." *Sci Adv* 7, no. 2 (2021): eabd4058 doi:10.1126/sciadv.abd4058
24. Volpe G, and Volpe G. "The Topography of the Environment Alters the Optimal Search Strategy for Active Particles." *Proc Natl Acad Sci USA* 114, no. 43 (2017): 11350–5. doi:10.1073/pnas.1711371114
25. Joeri AJ W, Mytiliniou M, Falko CHde W, Reuvers TGA, Holcman D, and Heinrich D. "Chemotaxis and Topotaxis Add Vectorially for Amoeboid Cell Migration." *bioRxiv* (2019): 735779 doi:10.1101/735779
26. Schakenraad K, Ravazzano L, Sarkar N, Joeri AJ W, Merks RMH, and Giomi L. "Topotaxis of Active Brownian Particles." *Phys Rev E* 101, no. 3 (2020): 032602 doi:10.1103/physreve.101.032602
27. Masoliver J, Lindenberg K, Weiss GH, and Weiss. "A Continuous-Time Generalization of the Persistent Random Walk." *Physica A: Stat Mech its Appl* 157, no. 2 (1989): 891–898. doi:10.1016/0378-4371(89)90071-x
28. Zaburdaev V, Denisov S, and Klafter J. Lévy Walks. *Rev Mod Phys* 87, no. 2 (2015): 483, 530. doi:10.1103/revmodphys.87.483
29. Volpe G, Gigan S, and Volpe G. "Simulation of the Active Brownian Motion of a Microswimmer." *Am J Phys* 82, no. 7 (2014): 659–664. doi:10.1119/1.4870398
30. Jacobs K. "*Stochastic Processes for Physicists: Understanding Noisy Systems*". Cambridge, UK, Cambridge University Press, 2010. doi:10.1017/cbo9780511815980
31. Oliveira FA, Ferreira R, Lapas LC, and Vainstein MH. "Anomalous Diffusion: A Basic Mechanism for the Evolution of Inhomogeneous Systems." *Front Phys* 7 (2019): 18. doi:10.3389/fphy.2019.00018
32. Fuglede B, and Topsoe F. "Jensen-Shannon Divergence and Hilbert Space Embedding." In Proceedings of the 2004 International Symposium onInformation Theory, 2004. Chicago, Illinois, USA, p. 31. IEEE.
33. Viswanathan GM, Buldyrev SV, Havlin S, Da Luz MGE, Raposo EP, and Eugene Stanley H. "Optimizing the success of Random Searches." *nature* 401, no. 6756 (1999): 911-914. doi:10.1038/44831
34. Rens EG, and Edelstein-Keshet. L "From Energy to Cellular Forces in the Cellular Potts Model: An Algorithmic Approach." *PLoS Comput Biol* 15, no. 12 (2019): e1007459 doi:10.1371/journal.pcbi.1007459
35. Yang H, Gou X, Wang Y, Fahmy TM, Leung AY-H, Lu J, et al. "A Dynamic Model of Chemoattractant-Induced Cell Migration." *Biophysical J* 108, no. 7 (2015): 1645–51. doi:10.1016/j.bpj.2014.12.060
36. Niculescu I, Textor J, Rob J, and De Boer. "Crawling and Gliding: a Computational Model for Shape-Driven Cell Migration." *Plos Comput Biol* 11, no. 10 (2015): e1004280. doi:10.1371/journal.pcbi.1004280
37. Kim M-C, Silberberg YR, Abeyaratne R, Kamm KRD, and Asada HH. "Computational Modeling of Three-Dimensional ECM-Rigidity Sensing to Guide Directed Cell Migration." *Proc Natl Acad Sci USA* 115, no. 3 (2018): E390–E399. doi:10.1073/pnas.1717230115
38. Bechinger C, Di Leonardo R, Löwen H, Reichhardt C, Volpe G, and Volpe G. "Active Particles in Complex and Crowded Environments." *Rev Mod Phys* 88, no. 4 (2016): 045006 doi:10.1103/revmodphys.88.045006
39. Dimidov C, Oriolo G, and Trianni V. "Random Walks in Swarm Robotics: an experiment with Kilobots." In International Conference on Swarm Intelligence, pp. 185–196. Springer, Padma Resort Legian, Indonesia, 2016. doi:10.1007/978-3-319-44427-7_16
40. Katanov D, Gompper G, and Fedosov DA. Microvascular Blood Flow Resistance: Role of Red Blood Cell Migration and Dispersion." *Microvasc Res* 99 (2015): 57–66. doi:10.1016/j.mvr.2015.02.006
41. Tichet M, Prod'Homme V, Fenouille N, Ambrosetti D, Mallavialle A, Cerezo M, et al. "Tumour-derived SPARC Drives Vascular Permeability and Extravasation through Endothelial VCAM1 Signalling to Promote Metastasis." *Nat Commun* 6, no. 1 (2015): 1–15. doi:10.1038/ncomms7993
42. Mrass P, Rao Oruganti S, Fricke GM, Tafoya J, Byrum JR, Yang L, et al. "ROCK Regulates the Intermittent Mode of Interstitial T Cell Migration in Inflamed Lungs." *Nat Commun* 8, no. 1 (2017): 1–14. doi:10.1038/s41467-017-01032-2
43. Van H, and Peter JM. "A Model for a Correlated Random Walk Based on the Ordered Extension of Pseudopodia." *Plos Comput Biol* 6, no. 8 (2010): e1000874. doi:10.1371/journal.pcbi.1000874
44. Sarvaharman SS, Robles AH, and Giuggioli L. From Micro-to-macro: How the Movement Statistics of Individual Walkers Affect the Formation of Segregated Territories in the Territorial Random Walk Model. *Front Phys* 7 (2019): 129. doi:10.3389/fphy.2019.00129

Conflict of Interest: The authors declare that the research was conducted in the absence of any commercial or financial relationships that could be construed as a potential conflict of interest.